Time-resolved quasiparticle dynamics of the itinerant antiferromagnet $UPtGa_5$

Elbert E. M. Chia

Division of Physics and Applied Physics, School of Physical and Mathematical Sciences, Nanyang Technological University, Singapore 637371, Singapore

Jian-Xin Zhu, D. Talbayev,* H. J. Lee,† Namjung Hur,‡ N. O. Moreno,§ R. D. Averitt,‖ J. L. Sarrao, and A. J. Taylor

Los Alamos National Laboratory, Los Alamos, New Mexico 87545, USA

(Received 9 June 2011; revised manuscript received 26 October 2011; published 11 November 2011)

Time-resolved photoinduced reflectivity is measured in the spin-density-wave phase of the itinerant antiferromagnet $UPtGa_5$. Two relaxation components were seen: (a) a slow component whose amplitude appears below T_N, and relaxation time τ_{slow} exhibits an upturn near T_N, and (b) the fast component persists at all temperatures, with the relaxation time τ_{fast} also exhibiting an upturn near T_N. Comparing with pump-probe data on $UNiGa_5$, the differences are explained in the context of $UPtGa_5$ having A-type (rather than G-type) antiferromagnetism, resulting in partial Fermi surface nesting, partial gapping, and consequently finite density of states at the Fermi surface.

DOI: 10.1103/PhysRevB.84.174412 PACS number(s): 78.47.−p, 75.25.−j, 75.30.Fv

I. INTRODUCTION

The quasiparticle (QP) dynamics of the spin-density-wave (SDW) phase is an important area of study, especially in the high-temperature superconductors, where superconductivity and antiferromagnetism could coexist, either in an applied magnetic field[1,2] or in zero field.[3] In single-layered cuprates, where there is only a single layer of CuO_2 plane in the unit cell, antiferromagnetism is necessarily G type, where the nearest-neighbor spins in the CuO_2 plane are antiferromagnetically aligned. However, in multilayered cuprates, two types of antiferromagnetism can occur on the CuO_2 planes: (1) G-type antiferromagnetism or (2) A-type antiferromagnetism, that is, spins are ferromagnetically aligned along each plane, but antiferromagnetically aligned in adjacent planes. Being able to elucidate the magnetic alignment of the spins in multilayered cuprate superconductors in the coexistence phase is crucial in narrowing down the starting point for a pairing theory in high-temperature superconductivity. It is therefore important to study the QP dynamics of pure SDW systems before proceeding to more complex coexistence phases in the cuprate superconductors. At present there have been no systematic measurements of the QP dynamics of the SDW phase, *as a function of the type of antiferromagnetism*, where below the Néel temperature T_N, a SDW gap might open up.

Usually the SDW state in itinerant antiferromagnets is probed by techniques such as resistivity, specific heat, and neutron scattering. In resistivity and specific heat, a feature appearing at the Néel temperature T_N, such as a hump or peak, has been interpreted as due to the formation of a SDW gap Δ_{SDW}, and the accompanying partial (or total) disappearance of the Fermi surface (see, for example, Refs. 4–6). To determine the arrangement of spins inside the unit cell, however, requires the powerful technique of neutron scattering to measure the antiferromagnetic modulation vector Q.[7]

Ultrafast optical spectroscopy has recently been used in the study of correlated electron materials.[8–16] For example, in the heavy fermion $YbAgCu_4$,[8] time-resolved photoinduced reflectivity ($\Delta R/R$) measurements display a divergence of the electron-phonon relaxation time τ at the lowest temperatures. In another heavy fermion $Yb_{14}MnSb_{11}$, the coupling between an optical phonon mode and the Kondo effect was observed.[9] In cuprate,[10–12] pnictide,[13] and actinide[14] superconductors, charge-density-wave materials like $K_{0.3}MoO_3$,[15] and G-type itinerant antiferromagnet $UNiGa_5$,[17] τ diverges near T_c (or T_N) when a gap opens in the QP density of states (DOS). The temperature dependence of the relaxation time and peak amplitude has been explained by the phenomenological Rothwarf-Taylor (RT) model.[18] This model describes the relaxation of photoexcited superconductors, where the presence of a gap in the QP DOS gives rise to a relaxation bottleneck for carrier relaxation, arising from the competition between QP recombination and pair breaking by phonons.[19]

In addition, ultrafast optical spectroscopy was able to detect the presence of various order parameters in a sample, and whether these order parameters coexist or compete with one another.[20] For example, in the cuprate superconductor $Tl_2Ba_2Ca_2Cu_3O_y$ (Tl-2223, $T_c \sim 120$ K), superconductivity was suppressed by antiferromagnetism below $T_N \sim 40$ K.[12] In another overdoped cuprate $Bi_2Sr_2CaCu_2O_{8+\delta}$ (Bi-2212, $T_c \sim 65$ K), both the superconducting gap and pseudogap coexist in the superconducting state.[21] In the underdoped pnictide superconductor $(Ba,K)Fe_2As_2$, we see the interplay among SDW, bulk superconductivity, as well as precursor superconductivity at low temperatures.[13] Contrast this with neutron scattering, which is able to measure Q, yet cannot tell us the possible competition between antiferromagnetism and other order parameters. In addition to earlier ultrafast work done on the G-type antiferromagnet $UNiGa_5$,[17] it is therefore important to study the QP dynamics of an A-type antiferromagnet.

In this paper we investigate the QP response in the SDW state of the itinerant A-type antiferromagnet $UPtGa_5$. Unlike in $UNiGa_5$, where $\Delta R/R$ recovers completely within 20 ps via a single-exponential relaxation,[17] two relaxation components were seen in $UPtGa_5$: (a) The slow component appears only below T_N—its amplitude A_{slow} is BCS-like, and the relaxation time τ_{slow} exhibits an upturn near T_N; and (b) the fast component persists at all temperatures—A_{fast} is temperature

independent below T_N, with τ_{fast} also exhibiting an upturn near T_N. These data are explained in the context of $UPtGa_5$ having A-type (rather than G-type) antiferromagnetism. Its value of the SDW modulation vector $(0,0,\pi)$ results in the Fermi surface being partially gapped (rather than almost fully gapped, as in $UNiGa_5$). QP relaxation thus takes place via the gapped and gapless regions of the Fermi surface—relaxation via the gapped regions gives rise to the slow component, while relaxation via the gapless regions gives rise to the fast (metallic) component. Above T_N only the fast component remains. We fitted A_{slow} and τ_{slow} using the RT model. We further substantiate our claim by performing a realistic microscopic calculation on a tetragonal lattice in the SDW state of *both* $UNiGa_5$ and $UPtGa_5$—the QP DOS of the former shows a well-defined gap at the Fermi level, while the QP DOS of the latter is only slightly depressed. We have thus shown ultrafast optical spectroscopy to be able to distinguish between fully gapped and partially gapped SDW materials.

II. EXPERIMENTAL DETAILS

$UPtGa_5$ is a $5f$ itinerant antiferromagnet with $T_N \approx 26$ K. Its antiferromagnetic phase is A type with $Q = (0,0,\pi)$, compared to $Q = (\pi,\pi,\pi)$ in G-type $UNiGa_5$.[7] Its electronic specific heat coefficient $\gamma = 57$ mJ/mol K^2, similar to 30 mJ/mol K^2 in $UNiGa_5$.[4,5] Single crystals of $UPtGa_5$ were grown in Ga flux,[22] with dimensions $\sim 1 \times 1 \times 0.4$ mm^3. Specific heat measurements were performed in a Quantum Design PPMS from 2 to 300 K to determine T_N. In our experiment, an 80-MHz Ti:sapphire laser produces 50 fs pulses at ≈800 nm (1.5 eV) as the source of both pump and probe pulses, which were cross polarized. The pump spot diameter was 60 μm and that of probe was 30 μm. The reflected probe beam was focused onto an avalanche photodiode detector. The photoinduced change in reflectivity $(\Delta R/R)$ was measured using lock-in detection. In order to minimize noise, the pump beam was modulated at 1 MHz with an acousto-optical modulator. The pump power is 0.5 mW (compare this with 7 mW pump power for $UNiGa_5$ in Ref. 17), giving a pump fluence of ~ 0.3 μJ/cm^2 and a photoexcited QP density of $\sim 1 \times 10^{-3}$/unit cell, showing that the system is in the weak perturbation limit. The probe intensity was 10 times lower. Data were taken from 7 to 300 K. The photoinduced temperature rise at the lowest temperature was estimated to be ~3 K (accounted for in all data plots).

III. DATA ANALYSIS AND DISCUSSION

In Fig. 1 we show the time dependence of $\Delta R/R$ of $UPtGa_5$ below and above T_N. Below T_N two relaxation components were observed: a fast component (0.5–2 ps) which persists above T_N, and a slow one (20–~200 ps) that persists to slightly above T_N, possibly due to fluctuation effects. Data below T_N were fitted using two exponentials: $\Delta R/R = A_0 + A_{\text{slow}} \exp[-(t-t_0)/\tau_{\text{slow}}] + A_{\text{fast}} \exp[-(t-t_0)/\tau_{\text{fast}}]$, where t_0, the time delay of the first point of the fit, was included to ensure the fitted values of A_{fast} and A_{slow} were not skewed by the different rise-time dynamics at different temperatures. Data above T_N were fitted by one exponential.

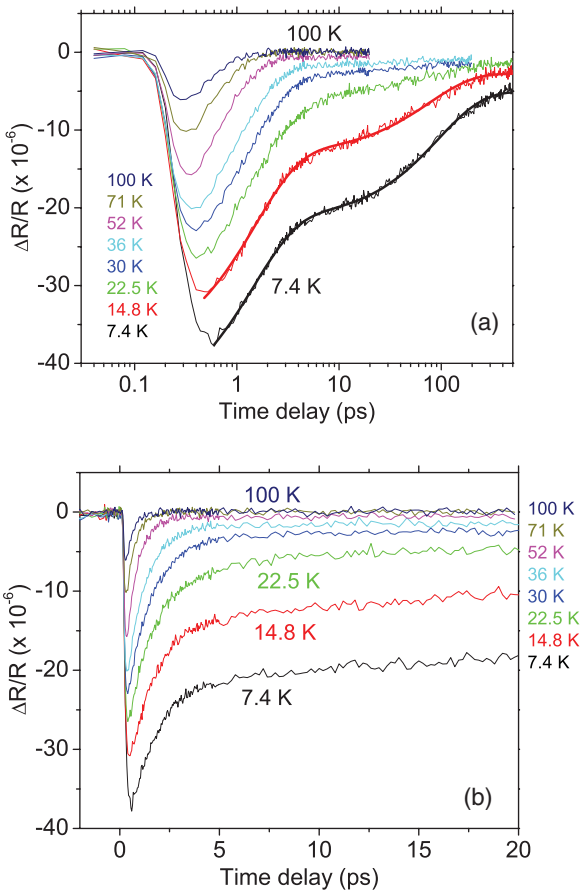

FIG. 1. (Color online) Transient reflection $\Delta R/R$ after photoexcitation by a 50 fs laser pulse above and below T_N for $UPtGa_5$. (a) For time delays up to 500 ps (logarithmic scale). (b) Blowup of data at short time delays up to 20 ps. Thick black (red) curves denote two-exponential fits of data at $T = 7.4$ K (14.8 K).

Figure 2 shows the temperature dependence of the relaxation amplitudes and relaxation times extracted from Fig. 1. Unlike in $UNiGa_5$, where there is only a single fast relaxation component,[17] here in $UPtGa_5$ two relaxation components were observed: (a) The slow component appears below T_N, and disappears slightly above T_N—its amplitude $A_{\text{slow}}(T)$ is BCS-like, and the relaxation time τ_{slow} exhibits an upturn neat T_N; and (b) the fast component persists at all temperatures, with τ_{fast} also exhibiting an upturn near T_N. Since the slow component vanishes around T_N, we associate it with QP relaxation across the "gapped" portions of the Fermi surface. The fast component then is associated with relaxation across the gapless portions of the Fermi surface.

We use the RT model to explain our data for the slow component.[18] It is a phenomenological model used to describe the relaxation of photoexcited superconductors, where the presence of a gap in the electronic DOS gives rise to a bottleneck for carrier relaxation. When two QPs with energies $\geqslant \Delta$ recombine (Δ is the superconducting gap magnitude), a high-frequency boson (HFB) with energy $\omega \geqslant 2\Delta$ is created. The HFBs that remain in the excitation volume can subsequently break additional Cooper pairs effectively inhibiting QP recombination. Recovery of superconductivity is thus governed by the decay of the HFB population. The RT analysis

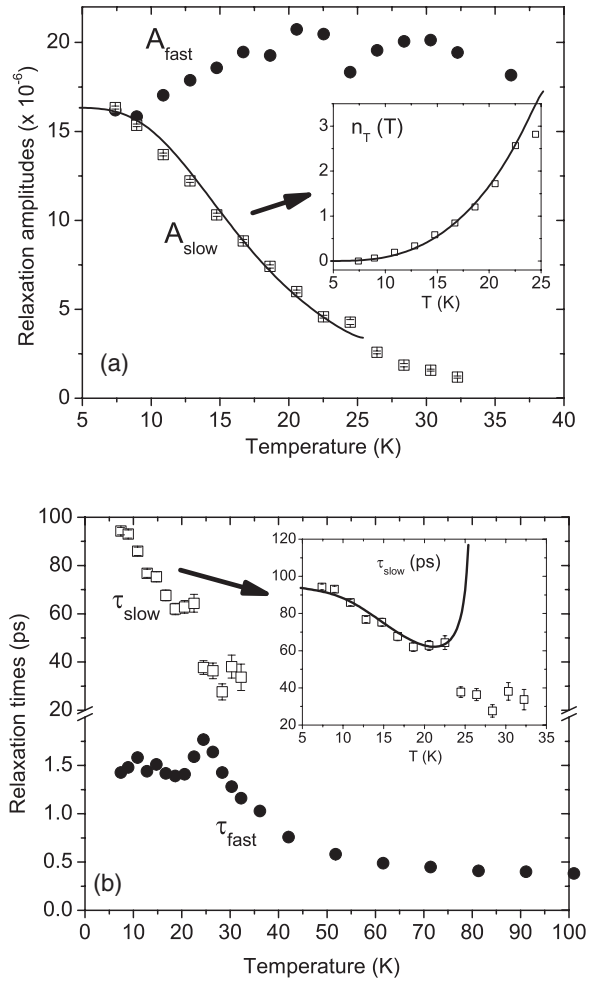

FIG. 2. (a) Temperature dependence of relaxation amplitudes A_{fast} and A_{slow}, and thermally excited QP densities n_T (inset). Solid lines are fits using the RT model. (b) Temperature dependence of relaxation times τ_{fast} and $A\tau_{\text{slow}}$. Solid line is the fit using the RT model.

for a material with a single energy gap, is as follows:[23] from the temperature dependence of the amplitude A, one obtains the density of thermally excited QPs n_T via $n_T \propto \mathcal{A}^{-1}-1$, where $\mathcal{A}(T)$ is the normalized amplitude $[\mathcal{A}(T=) A(T)/A(T\rightarrow 0)]$. Then we can fit the n_T data to the QP density per unit cell

$$n_T \propto \sqrt{\Delta(T)T}\exp[-\Delta(T)/T], \tag{1}$$

with $\Delta(0)$ as a fitting parameter and $\Delta(T)$ obeying a BCS temperature dependence. Moreover, for a constant pump intensity, the temperature dependence of n_T also governs the temperature dependence of the relaxation time τ given by[17,19,23]

$$\tau^{-1}(T) = \Gamma[\delta + 2n_T(T)](\Delta + \alpha T\Delta^4), \tag{2}$$

where Γ, δ, and α are temperature-independent fitting parameters, with α having an upper limit of $52/(\theta_D^3 T_{\min})$, θ_D being the Debye temperature, and $T_{\min}$ the minimum temperature of the experiment.

We then fit the data for the slow component (A_{slow} and τ_{slow}). That is, from $A_{\text{slow}}(0)$ and $A_{\text{slow}}(T)$ we obtain n_T [squares in the inset of Fig. 2(a)]. A fit of $n_T(T)$ at low temperatures to Eq. (1) yields $\Delta_0 = 1.76k_BT_N$, agreeing with the BCS weak-coupling value. Finally, we insert the fitted values of $n_T(T)$ into Eq. (2) to fit the experimental values of τ_{slow}, as shown in the inset of Fig. 2(b). The good fit shows that the slow component can be described by assuming QPs relaxing across a gap on some portions of the Fermi surface.

IV. THEORETICAL CALCULATIONS

A. Model calculation

We next perform two theoretical calculations—one model and another realistic, to justify our assertion that, in $UPtGa_5$, there exist *both* gapped and gapless portions of the Fermi surface. That is, we calculate the temperature dependence of the SDW gap as a function of the SDW modulation vector Q. We start with the model calculation: the model Hamiltonian for the SDW can be expressed as

$$\mathcal{H} = \sum_{\mathbf{k},\sigma}\epsilon_{\mathbf{k}}c^{\dagger}_{\mathbf{k}\sigma}c_{\mathbf{k}\sigma} + \frac{U}{N}\sum_{\mathbf{k},\mathbf{k}'}c^{\dagger}_{\mathbf{k}\uparrow}c_{\mathbf{k}'\uparrow}c^{\dagger}_{\mathbf{k}'+\mathbf{Q}\downarrow}c_{\mathbf{k}+\mathbf{Q}\downarrow}, \tag{3}$$

where $c^{\dagger}_{\mathbf{k}\sigma}(c_{\mathbf{k}\sigma})$ is the creation (annhilation) operator of an electron having the wave number $\mathbf{k}$ and spin σ. The first term represents the one-electron energy with dispersion $\epsilon_{\mathbf{k}}$, which, for a tetragonal crystal lattice, is given by

$$\epsilon_{\mathbf{k}} = -2t(\cos k_x a + \cos k_y a + \cos k_z c), \tag{4}$$

where t is the overlap integral between the $5f$ wave functions on neighboring sites, and a and c are lattice spacings. The second term in $\mathcal{H}$ denotes the on-site Coulomb interaction, with U being the on-site Coulomb energy, and N the number of lattice sites.

We define the SDW order parameter M_Q,

$$M_Q \equiv \frac{-U}{N}\sum_{\mathbf{k}}\langle c^{\dagger}_{\mathbf{k}+\mathbf{Q}\downarrow}c_{\mathbf{k}\uparrow}\rangle. \tag{5}$$

Then, after performing unitary transformation bilinearization and diagonalization we obtain the temperature dependence of M_Q in the following self-consistent equation:

$$M_Q = \frac{U}{N}\sum_{\mathbf{k}\in rBZ}\left\{\frac{-M_Q\,[f(E_+)-f(E_-)]}{\sqrt{\frac{1}{4}(\epsilon_{\mathbf{k}}-\epsilon_{\mathbf{k}+\mathbf{Q}})^2+M_Q^2}}\right\}, \tag{6}$$

where f is the Fermi function, the $\mathbf{k}$ points are taken from the reduced Brillioun zone (rBZ), and E_+ and E_- are the two branches of the one-particle energy in the SDW state given by

$$E_{\pm}(\mathbf{k}) = \frac{1}{2}(\epsilon_{\mathbf{k}}+\epsilon_{\mathbf{k}+\mathbf{Q}}) \pm \sqrt{\frac{1}{4}(\epsilon_{\mathbf{k}}-\epsilon_{\mathbf{k}+\mathbf{Q}})^2+M_Q^2}. \tag{7}$$

Figure 3 shows the temperature dependence of M_Q for $Q = (\pi,\pi,\pi)$ (solid circles) and $(0,0,\pi)$ (solid squares). U for each case is chosen such that the ratio $T_N[Q=(0,0,\pi)]/T_N[Q=(\pi,\pi,\pi)]$ is $\sim 26/85$. We see that the order parameter $M_Q(T)$ follows the BCS temperature dependence, as expected. This agrees with neutron scattering results of $UNiGa_5$ and $UPtGa_5$[7] (shown as "+" and "×" in Fig. 3), where the neutron scattering intensity is a measure of the sublattice magnetization M_Q.

For $UNiGa_5$ $[Q=(\pi,\pi,\pi)]$, $\epsilon_{\mathbf{k}} = -\epsilon_{\mathbf{k}-\mathbf{Q}}$ for most values of $\mathbf{k}$ in the rBZ, and so E_+ and E_- are separated by a

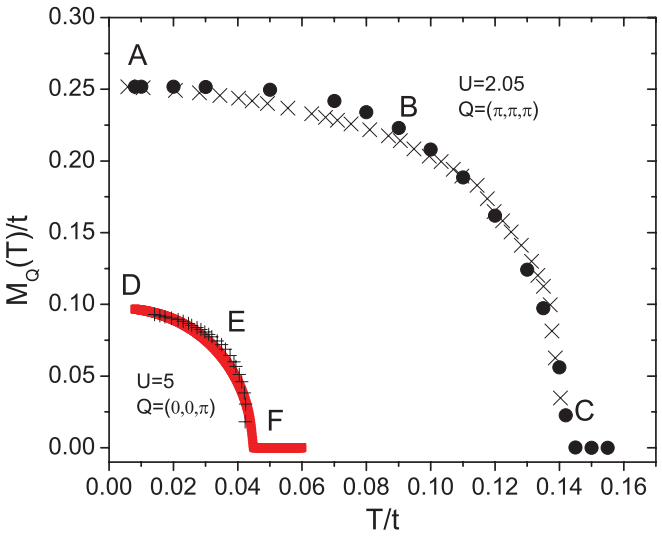

FIG. 3. (Color online) Calculated temperature dependence of the order parameter $M_Q(T)$ for a tetragonal lattice for $Q = (\pi,\pi,\pi)$ (solid circles), and $Q = (0,0,\pi)$ (solid squares). Experimental neutron scattering intensity for (+) $UPtGa_5$, and (×) $UNiGa_5$, taken from Ref. 7.

well-defined energy gap in most of **k** space. The SDW gap thus forms on the entire Fermi surface, resulting in a complete depression of the DOS at the Fermi level. QP relaxation then takes place across this SDW gap, resulting in a single-exponential relaxation. This agrees with our RT analysis of our data on $UniGa_5$.[17]

In $UPtGa_5$, however, $[Q = (0,0,\pi)]$. Here $\epsilon_{\mathbf{k}} \neq -\epsilon_{\mathbf{k}-\mathbf{Q}}$ in most of the rBZ. The SDW gap forms on only a small fraction of the Fermi surface due to partial nesting of the Fermi surface, and low-energy excitations can more easily occur on gapless parts of the Fermi surface. QP relaxation can thus take place on both the gapped and gapless regions of the Fermi surface, resulting in a two-component relaxation. The resultant (or total) DOS at the Fermi level is only slightly depressed. Being an *itinerant* antiferromagnet, $UPtGa_5$ becomes metallic above T_N, with $\tau_{\text{fast}} \sim 0.5$ ps. This value of τ_{fast} agrees with the relaxation time in metals such as Ag or Au,[24] strengthening our assertion that the fast relaxation in $UPtGa_5$ takes place across the *gapless* portions of the Fermi surface.

To further substantiate our claim, we calculate the DOS and its temperature dependence. DOS is a more accurate measure of the QP spectrum as it sums up the contributions from the entire (gapped *and* gapless) Fermi surface. It is given by

$$\rho(E) = \frac{-2}{N} \sum_{\mathbf{k}\in rBZ} \{f'[E - E_+(\mathbf{k})] + f'[(E - E_-(\mathbf{k})]\}, \quad (8)$$

where $f' \equiv \partial f(E)/\partial E$ accounts for thermal smearing, and the factor 2 for spin degeneracy. Note that in Eq. (8), f' becomes the δ function in the $T = 0$ limit. The resulting DOS is shown in Fig. 4, where the letters A–F represents the calculated DOS based on the values of T and $M_Q(T)$ in Fig. 3. The Fermi level is located at $E = 0$. For a $Q = (\pi,\pi,\pi)$ SDW material, illustrated in Fig. 4(a), a well-defined DOS gap develops below T_N, as evidenced by the sharp dips and coherence peaks appearing at $\pm M_Q$. With decreasing temperature, the dips

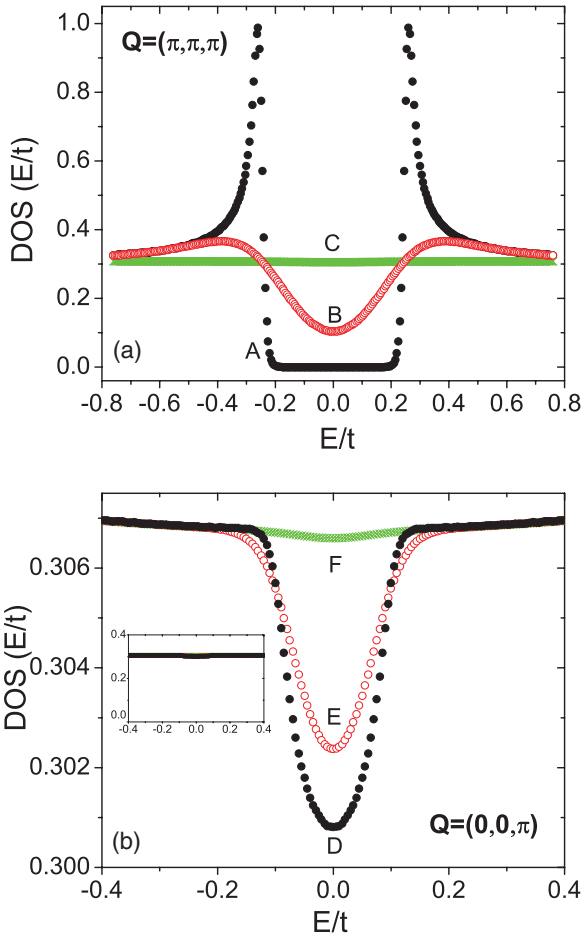

FIG. 4. (Color online) Calculated temperature dependence of the DOS in the SDW state for (a) $Q = (\pi,\pi,\pi)$, and (b) $Q = (0,0,\pi)$. The curves A–F represents DOS calculated from the values of T and $M_Q(T)$ in Fig. 3. $E = 0$ is the Fermi level.

approach zero, and the gaps are more well defined due to less thermal smearing. For $Q = (0,0,\pi)$, however, though dips do appear below T_N, the magnitude of the dips were very small ($\sim 10^{-3}$), even near $T = 0$. In the same scale as Fig. 4(a), it is almost flat, that is, energy independent, as shown in the inset of Fig. 4(b). We therefore conclude that in $UNiGa_5$ a well-defined gap in the DOS forms near the Fermi level in the SDW phase, whereas in $UPtGa_5$, DOS is only slightly depressed at the Fermi level.

B. Realistic band structure calculation

Next we perform a more realistic electronic structure calculation using the WIEN2k linearized augmented plane wave (LAPW) method,[25] based on density functional theory. A generalized gradient approximation[26] was used to treat exchange and correlation. Spin-orbit coupling was included in a second-variational way. The experimental lattice parameters for both $UNiGa_5$ and $UPtGa_5$[7] were used. The energy threshold to separate localized and delocalized electronic states was ~6 Ryd. The muffin-tin radii were $2.5a_0$ for uranium, $2.48a_0$ for nickel, $2.5a_0$ for platinum, and $2.2a_0$ (in $UNiGa_5$) and $2.28a_0$ (in $UPtGa_5$) for gallium, where a_0 is the Bohr radius. The criterion for the number of plane waves was

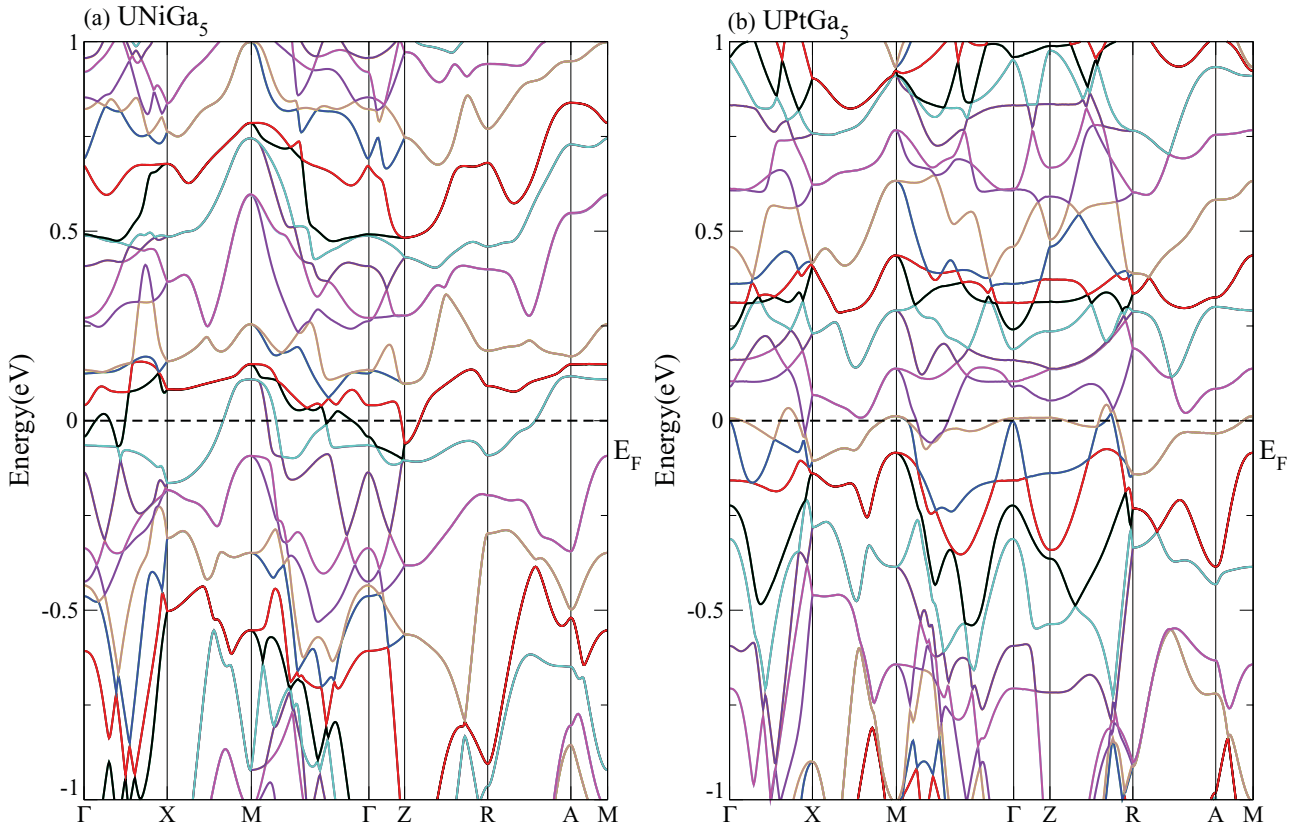

FIG. 5. (Color online) Band structure using the LAPW method of (a) $UNiGa_5$ and (b) $UPtGa_5$ in the SDW state. Notice the in $UPtGa_5$ a flat band runs between Γ and Z near the Fermi energy.

$R_{MT}^{\min} \times K^{\max} = 8$. The number of k points was at least 845 ($13 \times 13 \times 5$) for the self-consistency iteration, and 3600 ($20 \times 20 \times 9$) for the density of states calculations. An intrinsic lifetime broadening of 0.003 Ry was taken for the DOS calculations. In view of the fact that both $UNiGa_5$ and $UPtGa_5$ are itinerant antiferromagnetic metals, we treated U $5f$ as valence states. In addition, according to the experimental observation,[7] the magnetic order with propagation vectors $\mathbf{Q} = (1/2,1/2,1/2)$ for $UNiGa_5$ and $\mathbf{Q} = (0,0,1/2)$ for $UPtGa_5$ were taken, respectively.

Figure 5 shows the band structures of $UNiGa_5$ and $UPtGa_5$ in the SDW state. They confirm our expectation that there are more zero-energy QP states in $UPtGa_5$: First, its energy bands cut the Fermi energy at more $\mathbf{k}$ values. Second, a flat band exists along the line from Γ to Z near the Fermi energy—this van Hove singularity contributes a significant DOS at the Fermi energy. Note that in $UNiGa_5$ there are also bands cutting the Fermi energy, consistent with the fact that $UNiGa_5$ is an *itinerant* antiferromagnet, that is, antiferromagnetic metal. This also means that $UNiGa_5$ cannot be fully gapped in the SDW state, though the measure of its zero-energy QP states is still much smaller than in $UPtGa_5$. Figure 6 shows the total DOS of $UNiGa_5$ and $UPtGa_5$ in the SDW state, derived from Fig. 5. Notice that for $UNiGa_5$ [Fig. 6(a)], the DOS is strongly suppressed at the Fermi level—its QP gap is well defined, whose value is 97 meV (measured from the Fermi energy $E = 0$ to the location of the sharp coherent peak). Note however, that the suppression of the DOS is not complete, resulting in a small but nonzero DOS at the Fermi energy, consistent with our previous discussion of Fig. 5. In $UPtGa_5$ [Fig. 6(b)] its DOS is much larger at the Fermi energy, implying the existence of gapped (contributing zero DOS) and gapless (contributing nonzero DOS) portions of the Fermi surface.

It is worthwhile to make a few remarks: (1) for $UPtGa_5$ the profile of our calculated DOS as well as its intensity near the Fermi energy is in good agreement with that previously reported;[27] while for $UNiGa_5$ only the DOS intensity at the Fermi energy has been reported in literature,[28] and the value obtained here is smaller. The Sommerfeld coefficient $\gamma = 7.4\ \mathrm{mJ/K^2}$ mol is much smaller than that from the specific heat measurements ($\gamma \sim 50$–$64\ \mathrm{mJ/K^2}$ mol).[4,22] Overall the Sommerfeld coefficients obtained from the band structure calculations for both compounds are smaller than those values from the thermodynamic measurements. In view of the fact that the $UNiGa_5$ and $UPtGa_5$ single crystals used in experiments are of high sample quality, we ascribe the discrepancy to the inadequacy of the band structure theory. On the one hand, the local-density-type approximation usually gives a reasonable description of Fermi surface topology. On the other hand, the approximation underestimates the electronic correlations in d- and f-electron systems. We believe the quasiparticle renormalization effect due to electronic correlation should play an important role in enhancing the Sommerfeld coefficient. To fully resolve the disagreement, more theoretical work should be carried out in the future. (2) If we take the propogating wave vector for $UPtGa_5$ as $Q = (\pi,\pi,\pi)$, the obtained DOS

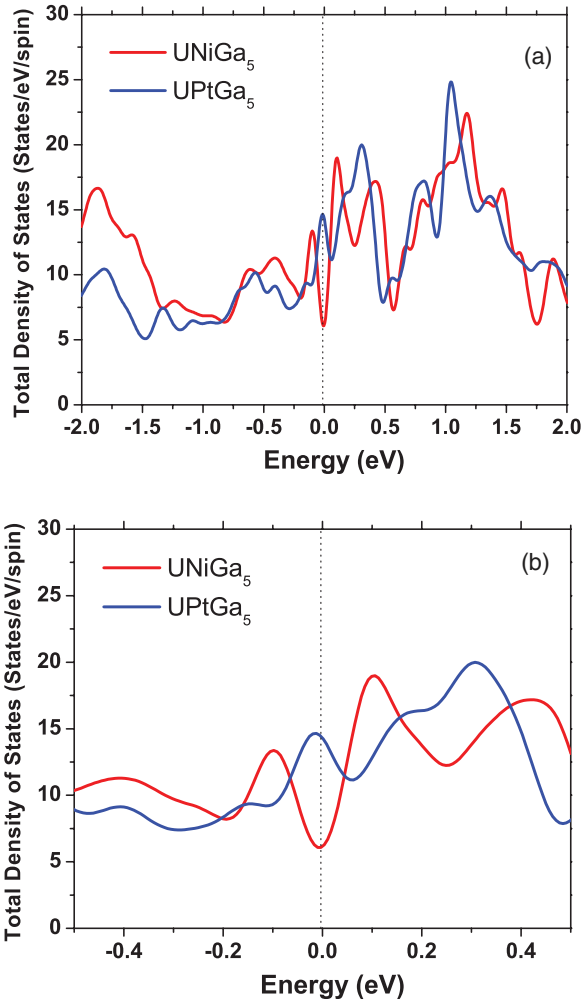

FIG. 6. (Color online) Total DOS calculated from the LAPW method for $UNiGa_5$ and $UPtGa_5$ in the magnetic unit cell in the energy range (a) (−2,2) eV and (b) (−0.5,0.5) eV. $E = 0$ is the Fermi level. Notice at the Fermi level DOS is strongly suppressed in $UNiGa_5$.

profile is quite similar to that of $UNiGa_5$, that is, a dip-like structure shows up at the Fermi energy. It indicates that the electronic structure difference between $UPtGa_5$ and $UNiGa_5$ is due to the difference of propgating vector $Q = (0,0,\pi)$ versus $Q = (\pi,\pi,\pi)$. It is intrinsic rather than a numerical artifact.

We note that, in the SDW iron pnictides such as $BaFe_2As_2$[13] and $SrFe_2As_2$,[29] only a single relaxation component is observed, despite the presence of gapless parts of the Fermi surface. The number of relaxation components in a material does not just depend on the number of subsystems that the electrons are coupled to. It also depends on whether these different subsystems are coupled to one another in any way. If these subsystems are coupled, then we would only see one relaxation component, with the relaxation time $1/\tau = \sum_{i=1}^{N} 1/\tau_i$, where τ_i is the characteristic time that the electrons transfer their energies to subsystem i, and N is the number of subsystems. On the other hand, if all the subsystems are uncoupled, then we should see N relaxation times. Since τ_{fast} also shows an upturn near T_N, it is possible that, in $UPtGa_5$, a multiband system, intraband scattering is so much stronger than interband scattering, that the electrons around different parts of the Fermi surface can be regarded as two separate subsystems. Hence two relaxation components are seen whose relaxation times exhibited an upturn at T_N.

V. CONCLUSION

We have performed time-resolved photoinduced reflectivity measurements in the SDW phase in the itinerant antiferromagnet $UPtGa_5$. Two relaxation components were seen: (a) a slow component whose amplitude appears below T_N and disappears around T_N, and relaxation time τ_{slow} exhibits an upturn near T_N; and (b) the fast component persists at all temperatures, with the relaxation time τ_{fast} also exhibiting an upturn near T_N. Comparing with pump-probe data on $UNiGa_5$, the differences are explained in the context of $UPtGa_5$ having A-type (rather than G-type) antiferromagnetism. Its value of the SDW modulation vector $(0,0,\pi)$ results in the Fermi level being partially gapped. QP relaxation thus takes place via the gapped and gapless regions of the Fermi surface—relaxation via the gapped regions gives rise to the slow component, while relaxation via the gapless regions gives rise to the fast (metallic) component. Our study thus extends the utility of ultrafast spectroscopy to study SDW materials of various modulation vectors Q.

ACKNOWLEDGMENTS

Work at Los Alamos was supported by the Los Alamos LDRD program. E. E. M. C. acknowledges support from the G. T. Seaborg Postdoctoral Fellowship, Singapore Ministry of Education Academic Research Fund Tier 1 (RG41/07) and Tier 2 (ARC23/08), as well as National Research Foundation Competitive Research Programme (NRF-CRP4-2008-04). We acknowledge H. Yamagami for useful discussions.

*Also at Department of Physics and Engineering Physics, Tulane University, New Orleans, LA 70118, USA.
†Also at Department of Physics, University of California at Berkeley, Berkeley, CA, USA.
‡Also at Department of Physics, Inha University, Incheon 402-751, South Korea.
§Also at Department of Physics, Federal University of Sergipe, São Cristovão, SE 49100-000, Brazil.
‖Also at Department of Physics, Boston University, Boston, MA, USA.

[1] B. Lake *et al.*, Nature (London) **415**, 299 (2002).
[2] H. J. Kang, P. Dai, J. W. Lynn, M. Matsuura, J. R. Thompson, S.-C. Zhang, D. N. Argyriou, Y. Onose, and Y. Tokura, Nature (London) **423**, 522 (2003).
[3] H. Mukuda, M. Abe, Y. Araki, Y. Kitaoka, K. Tokiwa, T. Watanabe, A. Iyo, H. Kito, and Y. Tanaka, Phys. Rev. Lett. **96**, 087001 (2006).

[4]Y. Tokiwa, Y. Haga, E. Yamamoto, D. Aoki, N. Watanabe, R. Settai, T. Inoue, K. Kindo, H. Harima, and Y. Onuki, J. Phys. Soc. Jpn. **70**, 1744 (2001).
[5]Y. Tokiwa, S. Ikeda, Y. Haga, T. Okubo, T. Iizuka, K. Sugiyama, A. Nakamura, and Y. Onuki, J. Phys. Soc. Jpn. **71**, 845 (2002).
[6]E. Fawcett, Rev. Mod. Phys. **60**, 209 (1988).
[7]Y. Tokiwa, Y. Haga, N. Metoki, Y. Ishii, and Y. Onuki, J. Phys. Soc. Jpn. **71**, 725 (2002).
[8]J. Demsar, R. D. Averitt, K. H. Ahn, M. J. Graf, S. A. Trugman, V. V. Kabanov, J. L. Sarrao, and A. J. Taylor, Phys. Rev. Lett. **91**, 027401 (2003).
[9]K. S. Burch, E. E. M. Chia, D. Talbayev, B. C. Sales, D. Mandrus, A. J. Taylor, and R. D. Averitt, Phys. Rev. Lett. **100**, 026409 (2008).
[10]S. G. Han, Z. V. Vardeny, K. S. Wong, O. G. Symko, and G. Koren, Phys. Rev. Lett. **65**, 2708 (1990).
[11]J. Demsar, B. Podobnik, J. E. Evetts, G. A. Wagner, and D. Mihailovic, Europhys. Lett. **45**, 381 (1999).
[12]E. E. M. Chia, J.-X. Zhu, D. Talbayev, R. D. Averitt, A. J. Taylor, K.-H. Oh, I.-S. Jo, and S.-I. Lee, Phys. Rev. Lett. **99**, 147008 (2007).
[13]E. E. M. Chia *et al.*, Phys. Rev. Lett. **104**, 027003 (2010).
[14]D. Talbayev *et al.*, Phys. Rev. Lett. **104**, 227002 (2010).
[15]J. Demsar, K. Biljakovic, and D. Mihailovic, Phys. Rev. Lett. **83**, 800 (1999).
[16]D. Talbayev, H. Zhao, G. Lupke, A. Venimadhav, and Q. Li, Phys. Rev. B **73**, 014417 (2006).
[17]E. E. M. Chia, J.-X. Zhu, H. J. Lee, N. Hur, N. O. Moreno, E. D. Bauer, T. Durakiewicz, R. D. Averitt, J. L. Sarrao, and A. J. Taylor, Phys. Rev. B **74**, 140409(R) (2006).
[18]A. Rothwarf and B. N. Taylor, Phys. Rev. Lett. **19**, 27 (1967).
[19]V. V. Kabanov, J. Demsar, and D. Mihailovic, Phys. Rev. Lett. **95**, 147002 (2005).
[20]E. E. M. Chia, J.-X. Zhu, D. Talbayev, and A. J. Taylor, Phys. Status Solidi RRL **5**, 1 (2011).
[21]S. K. Nair, X. Zou, E. E. M. Chia, J.-X. Zhu, C. Panagopoulos, S. Ishida, and S. Uchida, Phys. Rev. B **82**, 212503 (2010).
[22]N. O. Moreno, E. D. Bauer, J. L. Sarrao, M. F. Hundley, J. D. Thompson, and Z. Fisk, Phys. Rev. B **72**, 035119 (2005).
[23]J. Demsar, J. L. Sarrao, and A. J. Taylor, J. Phys. Condens. Matter **18**, R281 (2006).
[24]R. H. M. Groeneveld, R. Sprik, and A. Lagendijk, Phys. Rev. B **51**, 11433 (1995).
[25]P. Blaha, K. Schwarz, G. Madsen, D. Kvasnicka, and J. Luitz, *WIEN2k, An Augmented Plane Wave Plus Local Orbitals Program for Calculating Crystal Properties* (Vienna University of Technology, Austria, 2001).
[26]J. P. Perdew, K. Burke, and M. Ernzerhof, Phys. Rev. Lett. **77**, 3865 (1996).
[27]H. Yamagami, Acta Phys. Pol. B **34**, 1201 (2003).
[28]H. Yamagami, Physica B **312-313**, 297 (2002).
[29]L. Stojchevska, P. Kusar, T. Mertelj, V. V. Kabanov, X. Lin, G. H. Cao, Z. A. Xu, and D. Mihailovic, Phys. Rev. B **82**, 012505 (2010).